International Journal of Nanomedicine

Dovepress
open access to scientific and medical research

Open Access Full Text Article

ORIGINAL RESEARCH

Iodinated oil-loaded, fluorescent mesoporous silica-coated iron oxide nanoparticles for magnetic resonance imaging/computed tomography/fluorescence trimodal imaging

This article was published in the following Dove Press journal:
International Journal of Nanomedicine
21 May 2014
Number of times this article has been viewed

Sihan Xue[1]
Yao Wang[1]
Mengxing Wang[2]
Lu Zhang[1]
Xiaoxia Du[2]
Hongchen Gu[1]
Chunfu Zhang[1,3]

[1]School of Biomedical Engineering and Med-X Research Institute, Shanghai Jiao Tong University, [2]Shanghai Key Laboratory of Magnetic Resonance, Department of Physics, East China Normal University, [3]State Key Laboratory of Oncogenes and Related Genes, Shanghai Cancer Institute, School of Biomedical Engineering, Shanghai Jiao Tong University, Shanghai, People's Republic of China

Abstract: In this study, a novel magnetic resonance imaging (MRI)/computed tomography (CT)/fluorescence trifunctional probe was prepared by loading iodinated oil into fluorescent mesoporous silica-coated superparamagnetic iron oxide nanoparticles (i-fmSiO4@SPIONs). Fluorescent mesoporous silica-coated superparamagnetic iron oxide nanoparticles (fmSiO4@SPIONs) were prepared by growing fluorescent dye-doped silica onto superparamagnetic iron oxide nanoparticles (SPIONs) directed by a cetyltrimethylammonium bromide template. As prepared, fmSiO4@SPIONs had a uniform size, a large surface area, and a large pore volume, which demonstrated high efficiency for iodinated oil loading. Iodinated oil loading did not change the sizes of fmSiO4@SPIONs, but they reduced the MRI T2 relaxivity (r2) markedly. I-fmSiO4@SPIONs were stable in their physical condition and did not demonstrate cytotoxic effects under the conditions investigated. In vitro studies indicated that the contrast enhancement of MRI and CT, and the fluorescence signal intensity of i-fmSiO4@SPION aqueous suspensions and macrophages, were intensified with increased i-fmSiO4@SPION concentrations in suspension and cell culture media. Moreover, for the in vivo study, the accumulation of i-fmSiO4@SPIONs in the liver could also be detected by MRI, CT, and fluorescence imaging. Our study demonstrated that i-fmSiO4@SPIONs had great potential for MRI/CT/fluorescence trimodal imaging.

Keywords: multifunctional probe, SPIONs, mesoporous silica, iodinated oil

Introduction

Imaging techniques, such as magnetic resonance imaging (MRI), X-ray computed tomography (CT), fluorescence imaging, and positron emission tomography have been extensively applied for various disease diagnoses in the last few decades.[1,2] However, each imaging technique has its own advantages and disadvantages in the field of biomedical imaging. For example, CT can provide superior images of electron-dense materials, but it faces challenges in distinguishing between subtle changes in soft tissues due to their similar X-ray absorption.[3] MRI offers excellent soft tissue contrast and high spatial resolution, but it is not as sensitive as optical imaging.[4] Fluorescence imaging has high sensitivity, but its penetration depth and spatial resolution are low.[5] Therefore, a single modality is insufficient for diagnosis, and the information obtained from these three imaging modalities together could solve the problems of sensitivity and resolution that arise from the selection of a particular imaging modality.[6–9] In this context, the integration of multiple imaging components into a single structure enabling MRI/CT/fluorescence trimodal imaging has been of particular interest in recent years.

Correspondence: Chunfu Zhang
School of Biomedical Engineering and Med-X Research Institute, Shanghai Jiao Tong University, 1954 Huashan Road, Shanghai 200030, People's Republic of China
Tel +86 216 2933 323
Fax +86 216 293 2904
Email cfzhang@sjtu.edu.cn

To develop high-performance MRI/CT/fluorescence trimodal imaging agents, nanomaterials containing high atomic number components have often been prepared.[10] Hu et al[8] prepared a fluorescent gold nanocluster via the reduction of $HAuCl_4$ with bovine serum albumin. After labeling with gadolinium, the accumulation of a gadolinium–gold hybrid nanocluster in tumor tissues could be detected by MRI and CT, as well as by near-infrared fluorescent imaging. Recently, Dong et al[11] fabricated a novel Au nanoparticle-decorated, dye-doped superparamagnetic hybrid composite nanosphere for simultaneous MRI/CT/fluorescence imaging. Currently, in addition to hybrid nanomaterials, great effort has also been devoted to constructing high-quality lanthanide-doped up-conversion nanocrystals for multimodal imaging.[12] Due to these high atomic number components and unique optical properties, up-conversion nanocrystals have frequently been developed as imaging probes for MRI/CT/fluorescence trimodal imaging.[13–16]

However, serving as CT imaging components, clinically used iodinated compounds have been explored for the fabrication of multimodal imaging agents in only a few cases. Zheng et al[17,18] reported a liposome formulation that coencapsulated iohexol (a conventional iodine-based CT agent) and gadoteridol (a conventional gadolinium-based magnetic resonance [MR] agent) within their internal aqueous compartment as an MRI/CT dual modal contrast agent. The long in vivo lifetime circulation allowed for simultaneous CT and MR imaging.[17,18] Recently, Ding et al[6] developed a kind of quantum dots–iodinated oil nanoemulsion as a CT/fluorescence dual-modal contrast agent. The nanoemulsion could specifically target macrophages and visualize atherosclerotic plaques by clinical CT and fluorescence imaging.[6] However, to the best of our knowledge, there are no reports on the preparation of MRI/CT/fluorescence trimodal imaging agents based on clinically available iodinated compounds.

Previously, we have prepared mesoporous silica-coated superparamagnetic iron oxide nanoparticles (SPIONs), which proved to be effective carriers for small interfering ribonucleic acid.[19,20] Based on these studies, in the current study, we further developed fluorescent mesoporous silica-coated SPIONs (fmSiO4@SPIONs) by doping Cy5 dye into the silica walls, and we loaded the iodinated oil into the mesopores for the fabrication of a MRI/CT/fluorescence trifunctional contrast agent (i-fmSiO4@SPIONs). The potential of i-fmSiO4@SPIONs for MRI/CT/fluorescence trimodal imaging was explored both in vitro and in vivo.

Materials and methods

Materials

Methoxypolyethylene glycol succinimidyl propionate (molecular weight [MW]: 5,000) was obtained from Shanghai Yare Biotech, Inc. (Shanghai, People's Republic of China). Iodinated oil was bought from Guerbet (Villepinte, France). Cy5.5 N-hydroxysuccinimide (NHS) ester was purchased from GE Healthcare Life Sciences (Little Chalfont, UK). Other materials were purchased from Sigma-Aldrich Co. (St Louis, MO, USA).

Synthesis of fmSiO4@SPIONs

FmSiO4@SPIONs were synthesized via three steps: synthesis of Cy5 covalently-linked 3-aminopropyltriethoxysilane (APS) (Cy5-APS); synthesis of SPIONs; and coating SPIONs with fluorescent mesoporous silica. In brief, for the synthesis of Cy5-APS, 200 μg of Cy5.5-NHS was dissolved in 200 μL of APS solution, and the mixture was stirred for 24 hours in the dark prior to use. SPIONs were synthesized by a conventional coprecipitation method in aqueous phase and stabilized with oleic acid.[21] Briefly, ferric chloride hexahydrate ($FeCl_3\,6H_2O$; 24.0 g) and ferrous chloride tetrahydrate ($FeCl_2{\cdot}4H_2O$; 9.8 g) were dissolved in deionized water (100 mL) under a nitrogen atmosphere with vigorous stirring at 80°C. Fifty milliliters of ammonium hydroxide was then added rapidly into the solution and the solution turned black immediately. After 30 minutes, 3.8 g of oleic acid was added, and the reaction was kept at 80°C for 1.5 hours. Subsequently, the oleic acid-coated SPIONs were collected and washed with deionized water until neutral, and they were then transferred in situ into chloroform. The iron concentration of the resultant suspension was determined by inductively coupled plasma atomic emission spectroscopy and adjusted to 6.0 mg Fe/mL.

For the synthesis of fmSiO4@SPIONs,[22,23] the oleic acid-coated SPIONs (0.74 mL; 6.0 mg Fe/mL) were added to aqueous cetyltrimethylammonium bromide (CTAB) (Sigma-Aldrich) solution (5 mL, 0.08 M) and ultrasonicated for 0.5 hours to evaporate the chloroform, resulting in a transparent black dispersion. This dispersion was then added to a solution composed of water (35 mL), 3 mL of ethyl acetate and NH_4OH (0.7 mL, 28 wt%), followed by heating at 70°C for 10 minutes under stirring. Afterwards, tetraethoxysilane (0.5 mL) and Cy5-APS were introduced sequentially and dropwise to the reaction solution under stirring. After 10 minutes, APS (20 μL) was added and the solution was stirred for 3 hours. The as-synthesized particles were collected, and the template (CTAB) was removed

to generate mesopores by extraction of the surfactant using acetone as a solution. The final product was resuspended in ethanol.[24]

Modification of fmSiO4@SPIONs with PEG

The fmSiO4@SPIONs were modified with polyethylene glycol (PEG) to render them stable in plasma. For this purpose, an ethanol solution of the fmSiO4@SPIONs (10 mg) was mixed with 10 mg of methoxypolyethylene glycol succinimidyl propionate (MW 5,000) and dissolved in 10 mL of ethanol. The mixture was stirred for 3 hours at the ambient temperature to induce the formation of covalent bonds between the amine groups on the surface of fmSiO4@SPIONs and the succinimidyl groups of PEG. The PEG-modified fmSiO4@SPIONs were collected after washing them with ethanol and water in sequence to remove any unreacted PEG, and they were finally dispersed in phosphate buffered saline (PBS) (pH 7.4).

Characterizations of fmSiO4@SPIONs

Nitrogen sorption isotherms were measured at 77 K with a Micromeritics ASAP 2010 analyzer (Micromeritics Instruments Corporation, Norcross, GA, USA). The specific surface areas were calculated by the Brunauer–Emmett–Teller (BET) method[25] in a linear relative pressure range between 0.05–0.25. The pore size distributions were derived from the desorption branches of the isotherms by the nonlocal density functional theory[26] and Barrett–Joyner–Halenda (BJH) methods[27] using the Quantachrome Autosorb-1 software (Quantachrome Instruments, Boynton Beach, FL, USA). The morphology, size, and size distribution of the fmSiO4@SPIONs were characterized by transmission electron microscope (TEM) (JEOL JEM-2100F; JEOL, Tokyo, Japan) at an acceleration voltage of 200 kV. The particle size and size distribution were calculated using an image analysis program by measuring the diameter of no less than 300 particles. The zeta potentials were measured in water at pH 7.4 using a Zeta2000 Potential Analyzer (Malvern Instruments, Malvern, UK). The hydrodynamic diameters were determined by dynamic light scattering using a spectrometer (Autosizer 4700/PCS100; Malvern Instruments) equipped with an argon ion laser operating at 488 nm. Thermo gravimetric analysis of fmSiO4@SPIONs before and after PEG modification was performed with a NETZSCH TG 209 F1 iris instrument (NETZSCH-Feinmahltechnik GmbH, Selb, Germany) from room temperature to 900°C with a heating rate of 10°C/minute in a nitrogen flow (20 mL/minute). MR relaxometry of the magnetic particles was performed using a 1.41 T minispec mq60 nuclear MR (NMR) analyzer (Bruker Corporation, Billerica, MA, USA) and T2 relaxivity was deduced from inverse T2 as a function of iron concentrations.

Iodinated oil loading

For iodinated oil loading, various amounts of iodinated oil were dissolved into 1 mL of a mixture of ethanol and water (v/v=9:1) containing 1 mg of fmSiO4@SPIONs. After being vibrated for 4 hours at the ambient temperature, the iodinated oil-loaded fmSiO4@SPIONs (i-fmSiO4@SPIONs) were retrieved by a magnet, washed with water three times, and finally dispersed in PBS (pH 7.4). The loading efficiency, defined as the weight ratio of iodinated oil loaded to fmSiO4@SPIONs used (iodinated oil/fmSiO4@SPIONs, w/w), was evaluated by a spectrophotometric method using an ultraviolet spectrophotometer (NanoDrop 1000; Thermo Fisher Scientific, Waltham, MA, USA). The absorption of iodinated oil at 259 nm in the initial solution and the supernatant after loading was measured.

Release of iodinated oil

The possible release of iodinated oil from fmSiO4@SPIONs was also investigated. For this purpose, 10 mg of i-fmSiO4@SPIONs with a loading efficiency of 100% was suspended in 1 mL of water with different pH values (5.0, 7.4, and 9.0) at room temperature (25°C), or at different temperatures (4°C, 25°C, and 37°C) at pH 7.4 for different periods of time. The supernatants were collected after certain time intervals to determine the amount of iodinated oil released.

Phantom and cell imaging

To demonstrate the potential of i-fmSiO4@SPIONs for multimodal imaging, the MRI/CT/fluorescence imaging of the i-fmSiO4@SPION aqueous suspension at various concentrations or macrophages (RAW 264.7) incubated with different concentrations of i-fmSiO4@SPIONs for 3 hours was performed. For MRI and fluorescent imaging of the i-fmSiO4@SPION aqueous suspension, the concentrations of i-fmSiO4@SPIONs were 0.1 mg/mL, 0.2 mg/mL, 0.5 mg/mL, 1 mg/mL, and 2 mg/mL (in iron) with an iodinated oil loading efficiency of 100%. MRI was performed with a 3T MRI scanner (Trio Tim; Siemens AG, Munich, Germany) using a custom-made coil with a T2-weighted spin echo sequence (repetition time =2,000 ms; echo time =22.5 ms; field of view =60×60; matrix =256×256). For CT imaging, the concentrations of i-fmSiO4@SPIONs were 1 mg/mL, 5 mg/mL, 10 mg/mL, 50 mg/mL,

and 100 mg/mL. CT imaging was conducted with a preclinical micro-CT system (MicroXCT-200; Xradia Inc, Pleasanton, CA, USA). The following parameters were used: tube voltage =30 kVp; tube current =200 μA; resolution =2.5–3 μm; exposure time =15 seconds; distance of the X-ray tube to sample =35 mm; distance of the detector to sample =20 mm; slice thickness =1.83 μm; slice space =0; scan field of view =1.78 mm ×1.78 mm; pixel size =0.00183 mm; voxel =1.83 μm ×1.83 μm ×1.83 μm. Fluorescence imaging was performed with a GE fluorescence imaging system (eXplore Optix; GE Healthcare UK Ltd). For MRI and fluorescent imaging of the cells, macrophages were incubated with i-fmSiO4@SPIONs at concentrations of 0.1 mg/mL, 0.2 mg/mL, 0.5 mg/mL, 1 mg/mL, or 2 mg/mL (in iron), and cells (1×10^6) were suspended in PBS (pH 7.4; 100 μL). For CT imaging, macrophages were incubated with i-fmSiO4@SPIONs at concentrations of 1 mg/mL, 5 mg/mL, 10 mg/mL, 50 mg/mL, or 100 mg/mL (in iron), and cells (1×10^6) were suspended in 2% gelatin (100 μL) homogeneously. The imaging parameters were the same as those for phantom imaging.

Cytotoxicity of i-fmSiO4@SPIONs

The cytotoxicity of i-fmSiO4@SPIONs was evaluated with a human non-small-cell lung carcinoma cell line (H1299) and a human embryonic kidney 293 cell line (HEK293) using cell counting kit-8 (CCK-8; Dojindo Laboratories Co., Ltd., Kumamoto, Japan) according to the manufacturer's procedures.[28] For this purpose, the cells (1×10^4) were seeded in a 96-multiwell plate and incubated with i-fmSiO4@SPIONs with an iodinated oil-loading efficiency of 100% at different concentrations (5 mg/mL, 10 mg/mL, 50 mg/mL in iron) for different periods of time (1 hour, 3 hours, 5 hours, and 24 hours). After incubation, the culture medium was removed, and the cells were washed with PBS (pH 7.4) three times. Subsequently, fresh cell culture medium (90 μL) was added to each well, followed by the addition of a 10 μL CCK-8 solution. Then, the cells were incubated for 2 hours. The absorbance at 450 nm was recorded using a Wallace VICTOR3™ 1420 multilabel counter (PerkinElmer Inc., Waltham, MA, USA). Cell viability was expressed as the percentage of the absorbance of cells incubated with the nanoparticles to that of the cells maintained in normal culture medium.

In vivo MRI/CT/fluorescence imaging

The animal experiments were approved by the Animal Welfare Committee of Shanghai Jiao Tong University (Shanghai, People's Republic of China). All mice were housed in isolated cages with 12 hours light/dark cycle and fed with sterile food. To demonstrate the potential of i-fmSiO4@SPIONs for in vivo MRI/CT/fluorescence trimodal imaging, athymic nude mice were intravenously injected with i-fmSiO4@SPIONs with an iodinated oil-loading efficiency of 100% at the dose of 1 g/kg. CT, MRI, and fluorescence imaging were conducted at different periods of time postinjection. For MRI and fluorescence imaging, the imaging systems and parameters were the same as those for phantom and cell imaging. CT scans were conducted with a small-animal imaging system (Bioscan, Inc., Washington, DC, USA) and the images were reconstructed using InVivoScope (inviCRO, LLC, Boston, MA, USA).

Histological studies of liver

To identify i-fmSiO4@SPIONs present in the liver, the mice were sacrificed and dissected after imaging. Samples of liver were fixed with paraformaldehyde. Representative 5 μm thick sections were cut. Some liver sections were examined with fluorescent microscopy (Leica Microsystems, Wetzlar, Germany) and others were stained with Prussian blue. For Prussian blue staining, the slips were incubated with 10% Prussian blue for 5 minutes, 10% Prussian blue and 20% HCl (1:1) for 30 minutes, and counterstained with nuclear fast red for 5 minutes, successively.

Results and discussion

Since no single modality is perfect and sufficient in obtaining all the necessary information for a particular question, a combination of certain molecular imaging modalities can offer synergistic advantages over any modality alone.[29] MRI/CT/fluorescence trimodal imaging could ideally achieve exceptional soft tissue contrast by MRI, superior images of electron-dense materials by CT, and high sensitivity by fluorescent imaging.[30] Therefore, in this study, we fabricated a novel multifunctional probe by loading iodinated oil into fluorescent mesoporous silica-coated SPIONs (i-fmSiO4@SPIONs) (Figure 1A) and examined its potential for MRI/CT/fluorescence trimodal imaging. For the preparation of i-fmSiO4@SPIONs, SPIONs were first synthesized by coprecipitation of ferric and ferrous salts in basic condition. In order to achieve mesoporous silica coating, the SPIONs were made hydrophobic by surface coating with oleic acid. The size of the particles was around 8 nm. The mesoporous silica shells were subsequently coated with a silica sol–gel reaction of tetraethoxysilane in aqueous solution containing CTAB and SPIONs under basic conditions.[31–33] CTAB was used not only as the stabilizing

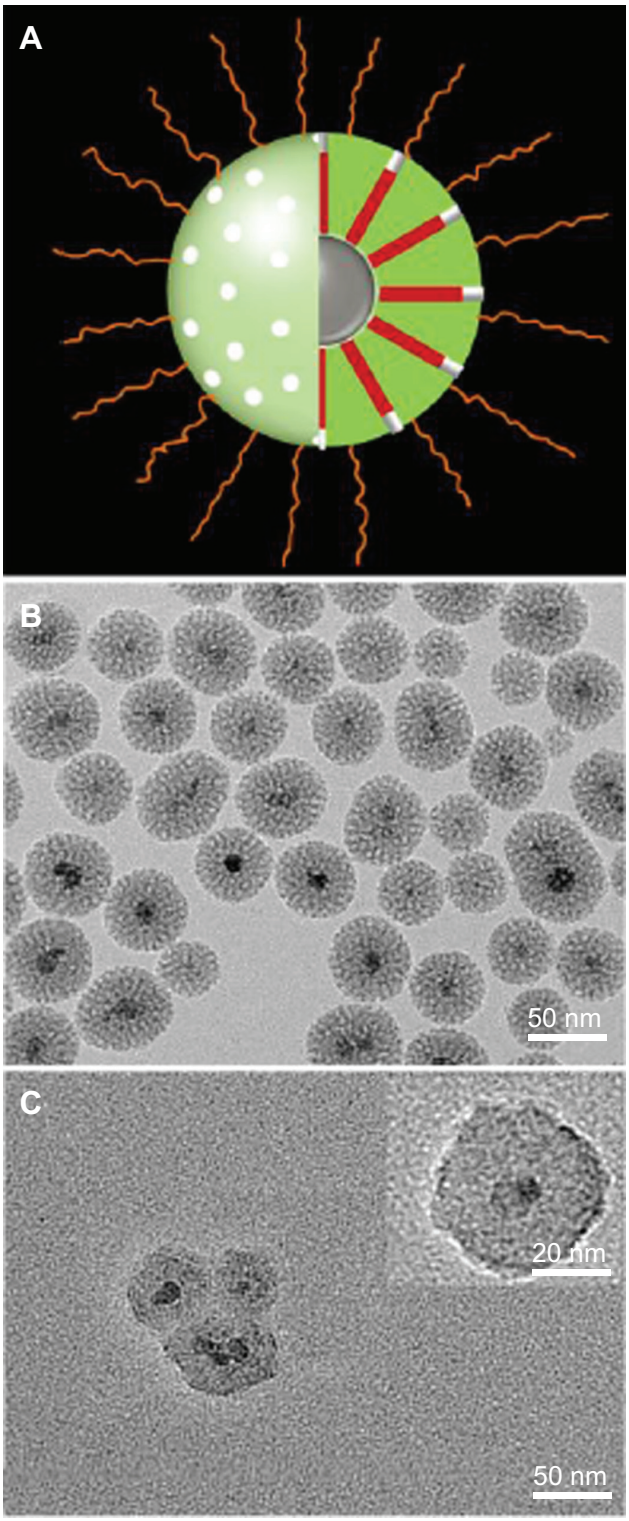

Figure 1 Schematic illustration of i-fmSiO4@SPIONs and TEM images of fmSiO4@SPIONs and i-fmSiO4@SPIONs.

Notes: (**A**) Schematic illustration of i-fmSiO4@SPIONs. TEM images of (**B**) fmSiO4@SPIONs and (**C**) i-fmSiO4@SPIONs. Insert: TEM image of i-fmSiO4@SPIONs with high magnification. After iodinated oil loading, the contrast between the silica walls and the pores disappeared.

Abbreviations: i-fmSiO4@SPIONs, iodinated oil-loaded fluorescent mesoporous silica-coated superparamagnetic iron oxide nanoparticles; TEM, transmission electron microscopy; fmSiO4@SPIONs, fluorescent mesoporous silica-coated superparamagnetic iron oxide nanoparticles.

agent in the transfer of hydrophobic SPIONs to the aqueous phase, but also as the organic structure-directing template that was used to establish mesopores on the silica shell. As indicated by TEM, fmSiO4@SPIONs were discrete and uniform in size, with a clear core–shell structure, and their average size was about 50 nm with a 20 nm mesoporous silica coating layer (Figure 1B). The mesoporous structure of fmSiO4@SPIONs was confirmed using nitrogen adsorption–desorption isotherms (Figure 2A). The pore size distribution calculated by the BJH model[27] showed that the mean value of the pore size was 2.7 nm, and it featured a narrow size distribution (Figure 2A), which demonstrated that fmSiO4@SPIONs had uniform porosity. The BET surface area[25] and total pore volume of fmSiO4@SPIONs were calculated to be 692.06 $m^2 g^{-1}$ and 1.68 $cm^3 g^{-1}$, respectively. These BET results indicated that fmSiO4@SPIONs were highly porous and had a large surface area. MR relaxometry of the fmSiO4@SPION water suspension was performed using a 1.41 T minispec mq60 NMR Analyzer (Bruker Corporation). T2 relaxivity (r_2) deduced from inverse T2 as a function of iron concentrations

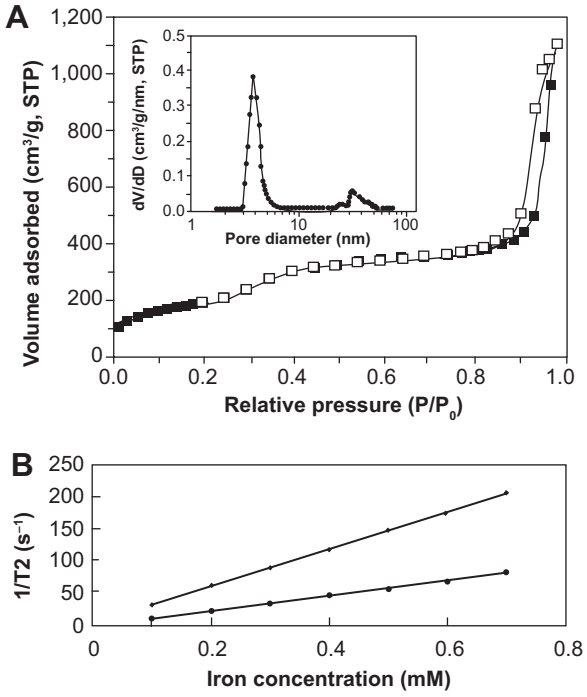

Figure 2 Nitrogen adsorption–desorption isotherms of fmSiO4@SPIONs, their pore size distribution, and the T2 relaxation rates of fmSiO4@SPIONs and i-fmSiO4@SPIONs.

Notes: (**A**) Nitrogen adsorption–desorption isotherms of fmSiO4@SPIONs; inset: pore size distribution; (**B**) T2 relaxation rates of fmSiO4@SPIONs and i-fmSiO4@SPIONs as the function of iron concentrations. T2 relaxivities were 288.70 $mM^{-1}s^{-1}$ for fmSiO4@SPIONs and 177.45 $mM^{-1}s^{-1}$ for i-fmSiO4@SPIONs.

Abbreviations: STP, standard temperature and pressure; fmSiO4@SPIONs, fluorescent mesoporous silica-coated superparamagnetic iron oxide nanoparticles; i-fmSiO4@SPIONs, iodinated oil-loaded fluorescent mesoporous silica-coated superparamagnetic iron oxide nanoparticles.

was 288.70 $mM^{-1}s^{-1}$ (Figure 2B). However, after iodinated oil loading, that was reduced to 111.45 $mM^{-1}s^{-1}$. Mesoporous silica coating slows diffusion of the water molecules confined in the mesopores. Moreover, hydrogen bonding between water and the mesoporous silica walls through Si–OH also restricts the mobility of water molecules. Considering the large surface area, hydrogen bonding would result in a large amount of immobilized water in the mesopores. The restriction of water mobility in the mesopores would lead to a longer time that the water molecules would experience the local magnetic field generated by the SPIONs, and thus more efficient dephasing (relaxation) of water protons would occur as a result. After iodinated oil loading, water molecules were excluded from the mesopores, which led to a reduction in T2 relaxivity. This observation was consistent with previous reports that mesoporous silica coating enhanced the MRI performance of SPIONs.[23,24] The zeta potentials of fmSiO4@SPIONs before and after PEG modification were +38.5±0.3 mV and +26.4±0.6 mV, respectively. Dynamic light scattering measurements revealed that the hydrodynamic sizes of fmSiO4@SPIONs in PBS (pH 7.4) were 149 nm before PEG modification and 174 nm after the modification (Figure 3A). PEG modification was further confirmed by thermogravimetric analysis, which indicated that PEG modification contributed to about a 13% weight loss of the modified fmSiO4@SPIONs (Figure S1).

Iodinated oil is an iodinated derivative of poppy seed oil, containing ethyl esters of linoleic, oleic, palmitic, and stearic acids with a high iodine content (30%–40% w/v) (Guerbet). Iodinated oil was first used as an intravascular embolizing

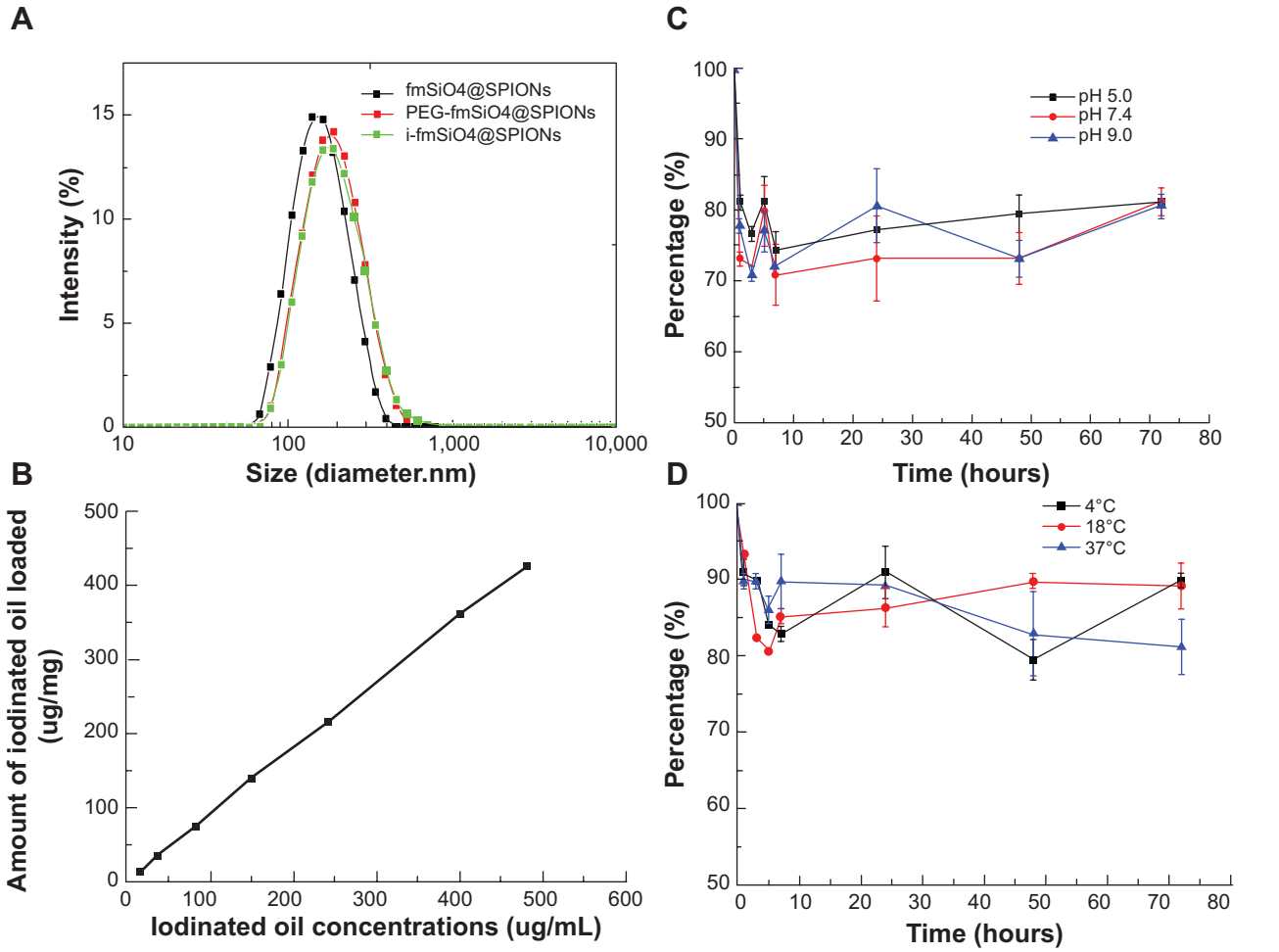

Figure 3 Hydrodynamic diameters of fmSiO4@SPIONs, PEG-modified fmSiO4@SPIONs, and i-fmSiO4@SPIONs in PBS, the iodinated oil loading capacity as the function of iodinated oil concentrations in a fmSiO4@SPION suspension, and the release of iodinated oil at different pH values and temperatures.

Notes: (**A**) Hydrodynamic diameters of fmSiO4@SPIONs, PEG-modified fmSiO4@SPIONs, and i-fmSiO4@SPIONs in PBS (pH 7.4). (**B**) Iodinated oil-loading capacity as the function of iodinated oil concentrations in a fmSiO4@SPION suspension (0.5 mg/mL). Release of iodinated oil at different (**C**) pH values and (**D**) temperatures. Ten milligrams of i-fmSiO4@SPIONs were suspended in 1 mL of water with different pH values (5.0, 7.4, and 9.0) at the ambient temperature (18°C), or at different temperatures (4°C, 18°C, and 37°C) at a pH of 7.4 for different periods of time.

Abbreviations: fmSiO4@SPIONs, fluorescent mesoporous silica-coated superparamagnetic iron oxide nanoparticles; PEG, polyethylene glycol; i-fmSiO4@SPIONs, iodinated oil-loaded fluorescent mesoporous silica-coated superparamagnetic iron oxide nanoparticles; PBS, phosphate buffered saline.

agent and lipid lymphographic contrast medium because of its hydrophobic nature and high viscosity.[34,35] To make it an injectable formulation, various nanoparticulate carriers, such as polymeric micelles, nanoemulsions, and liposomes, have been developed to encapsulate and transfer it into the aqueous phase.[36–38] Mesoporous silica materials have been intensively investigated for their potential application as delivery vehicles for small-molecule drugs, deoxyribonucleic acid, and proteins, owing to their uniform pore size, large surface area, and high accessible pore volume.[39–41]

Mesoporous silica-coated magnetic nanoparticles have been demonstrated to have great potential in both drug delivery and multimodal imaging.[32,42,43] Therefore, we speculated that fmSiO4@SPIONs may also be robust carriers for iodinated oil loading in the fabrication of an MRI/CT/fluorescence trimodal imaging agent. To load the iodinated oil into the mesopores, fmSiO4@SPIONs (1 mg) were suspended into a mixture of ethanol and water (v/v =9:1), into which various amounts of iodinated oil were subsequently dissolved. The loading capacity of fmSiO4@SPIONs almost linearly increased with increases in iodinated oil concentrations (Figure 3B). However, when too much iodinated oil was loaded, i-fmSiO4@SPIONs would flocculate and precipitate from the solution. Therefore, for in vitro and in vivo use, stability and iodinated oil loading efficiency should be carefully balanced. In the current study, fmSiO4@SPIONs with 100% loading efficiency were stable in PBS (pH 7.4), and they were used for further studies. Compared with fmSiO4@SPIONs, TEM images of i-fmSiO4@SPIONs revealed that iodinated oil was indeed loaded into the mesopores and the contrast between the pores and silica walls disappeared after loading (Figure 1C). The sizes of i-fmSiO4@SPIONs were similar to those of fmSiO4@SPIONs (about 50 nm, as measured by TEM and 174 nm, as measured by dynamic light scattering) (Figure 3A).

We also performed a release test of iodinated oil under different pH values (5.0, 7.4, and 9.0) at physiological temperature, or under different temperatures (4°C, 18°C, and 37°C) at pH 7.4. We found that there were burst releases of loaded iodinated oil during the initial 30 minutes (about 25%), and then no significant outflow of iodinated oil into the aqueous phase was observed during the remaining test period times for all the pH conditions (Figure 3C). There were also no significant differences in the release at each time point among the different pH conditions. The release trends were also observed at different temperatures (Figure 3D). The burst release may arise from the detachment of iodinated oil absorbed on the outer surface of the particles.

The cytotoxicity of i-fmSiO4@SPIONs was evaluated with a normal cell line (HEK293) and a cancerous cell line (H1299) at various i-fmSiO4@SPIONs concentrations (5 μg/mL, 10 μg/mL, and 50 μg/mL in iron) for different periods of time (1 hour, 3 hours, 5 hours, and 24 hours). As indicated in Figure 4, i-fmSiO4@SPIONs did not exert adverse effects on H1299 cells under the conditions investigated. For HEK293 cells, the cell viability was also not affected when the cells were incubated with i-fmSiO4@SPIONs for short periods of time. The viability was just slightly reduced when the cells were incubated for a relatively longer time (24 hours), reaching 96.24%±5.47%, 95.32%±4.62% and 94.61%±3.62% at concentrations of 5 μg/mL, 10 μg/mL, and 50 μg/mL (in iron), respectively. Regarding the cytotoxicity of mesoporous silica nanoparticles, a vast number of studies have been performed.[44,45] Although very different conclusions have been drawn depending on the type of mesoporous silica nanoparticles, it is believed that porosity, particle size, and postsynthetic treatment procedure (calcination/solvent extraction) may affect cytotoxicity.[46] Previously, we have observed that mesoporous silica-coated SPIONs had cytotoxic effects on neural progenitor cells (C17.2) when incubated with the particles at a concentration of 10 μg/mL (in iron) for 24 hours (viability: 76.62%±3.26%).[23] Although the cell tolerance of nanomaterials varied with the cell lines,[47–49] the improved biocompatibility of i-fmSiO4@SPIONs observed in this study may partially be due to iodinated oil loading, which filled the mesopores on the surface of fmSiO4@SPIONs.

Prior to in vivo imaging studies, we first checked the potentials of i-fmSiO4@SPIONs for MRI/CT/fluorescence trimodal imaging in vitro with aqueous solutions containing various concentrations of i-fmSiO4@SPIONs and macrophages (RAW 264.7) incubated with different concentrations of i-fmSiO4@SPIONs. The CT, fluorescence, and T2-weighted MR images showed that as the concentration of the i-fmSiO4@SPIONs increased, a brighter fluorescence of Cy5, and a darker CT and T2-weighted MR signal were observed (Figure 5A). For MR imaging, contrast enhancement was obvious when the i-fmSiO4@SPION concentration was 0.5 mg/mL, whereas it was 0.1 mg/mL for fluorescence imaging. For CT imaging, i-fmSiO4@SPIONs induced a contrast enhancement when the concentration was at least equal to 10 mg/mL (Figure 5A). These observations were consistent with previous reports, which noted that among these three imaging modalities, fluorescence imaging has the highest sensitivity, followed by MRI, and the contrast sensitivity of CT is the lowest.[5,50] When macrophages were

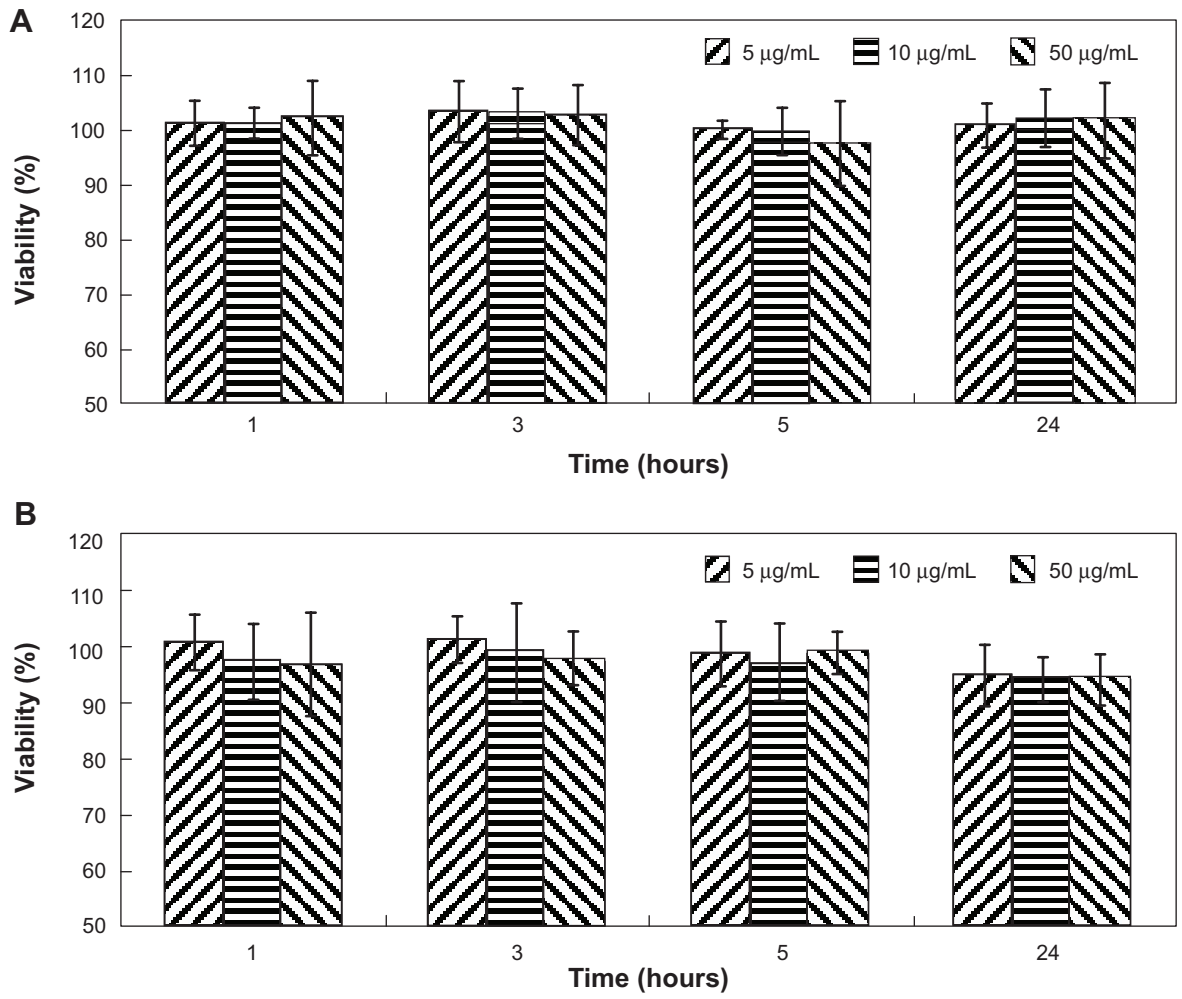

Figure 4 Viability of H1299 cells and HEK293 cells incubated with i-fmSiO4@SPIONs at different concentrations for different periods of time.
Notes: (**A**) H1299 cells and (**B**) HEK293 cells.
Abbreviation: i-fmSiO4@SPIONs, iodinated oil-loaded fluorescent mesoporous silica-coated superparamagnetic iron oxide nanoparticles.

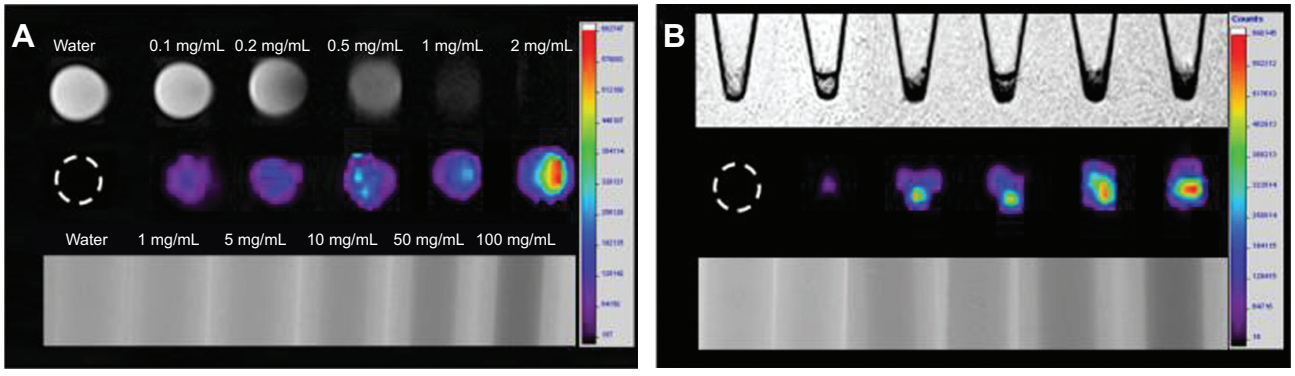

Figure 5 In vitro MRI/CT/fluorescence imaging of an i-fmSiO4@SPION aqueous suspension and macrophages incubated with i-fmSiO4@SPIONs at different concentrations (in iron).
Notes: (**A**) I-fmSiO4@SPION aqueous suspension and (**B**) macrophages. For the T2-weighted MRI (up) and fluorescent imaging (middle) of macrophages, the cells were incubated with i-fmSiO4@SPIONs at concentrations of 0 mg/mL, 0.1 mg/mL, 0.2 mg/mL, 0.5 mg/mL, 1 mg/mL, and 2 mg/mL (from left to right) for 3 hours. For CT imaging (down), the cells were incubated with i-fmSiO4@SPIONs at concentrations of 0 mg/mL, 1 mg/mL, 5 mg/mL, 10 mg/mL, 50 mg/mL, and 100 mg/mL (from left to right).
Abbreviations: MRI, magnetic resonance imaging; CT, computed tomography; i-fmSiO4@SPIONs, iodinated oil-loaded fluorescent mesoporous silica-coated superparamagnetic iron oxide nanoparticles.

incubated with i-fmSiO4@SPIONs, the cells would uptake the particles, which allowed us to examine the potential of i-fmSiO4@SPIONs in cell imaging. The MRI/CT/fluorescence trimodal imaging of the cells is shown in Figure 5B. The signal enhancement trends of MRI/CT/fluorescence trimodal imaging were similar to those observed in aqueous suspension of i-fmSiO4@SPIONs. With increases in the particle concentrations for cell incubation, brighter fluorescence and darker CT and T2-weighted MR signals were presented.

It is known that when nanoparticles are injected intravenously, parts of nanoparticles are sequestered by the liver through the reticuloendothelial system.[51,52] To investigate the potential of i-fmSiO4@SPIONs for in vivo imaging, we intravenously injected the i-fmSiO4@SPIONs into the nude mice (number =3) at the dose of 1 g/kg and obtained fluorescence, CT, and T2-weighted MR images of livers before injection and at 0.5 hours and 1 hour after injection (Figure 6). Half an hour following the injection, the accumulation of the nanoparticles in the liver could be detected in the T2-weighted MR images with marked decreases in MR signal intensity. The hypointense signal was more significant at 1 hour after the injection. For CT imaging, the contrast enhancement was also obvious 30 minutes postinjection, and it was further intensified at 1 hour after the injection. The trend of signal enhancement for fluorescence imaging was similar to those observed for CT and MRI. However,

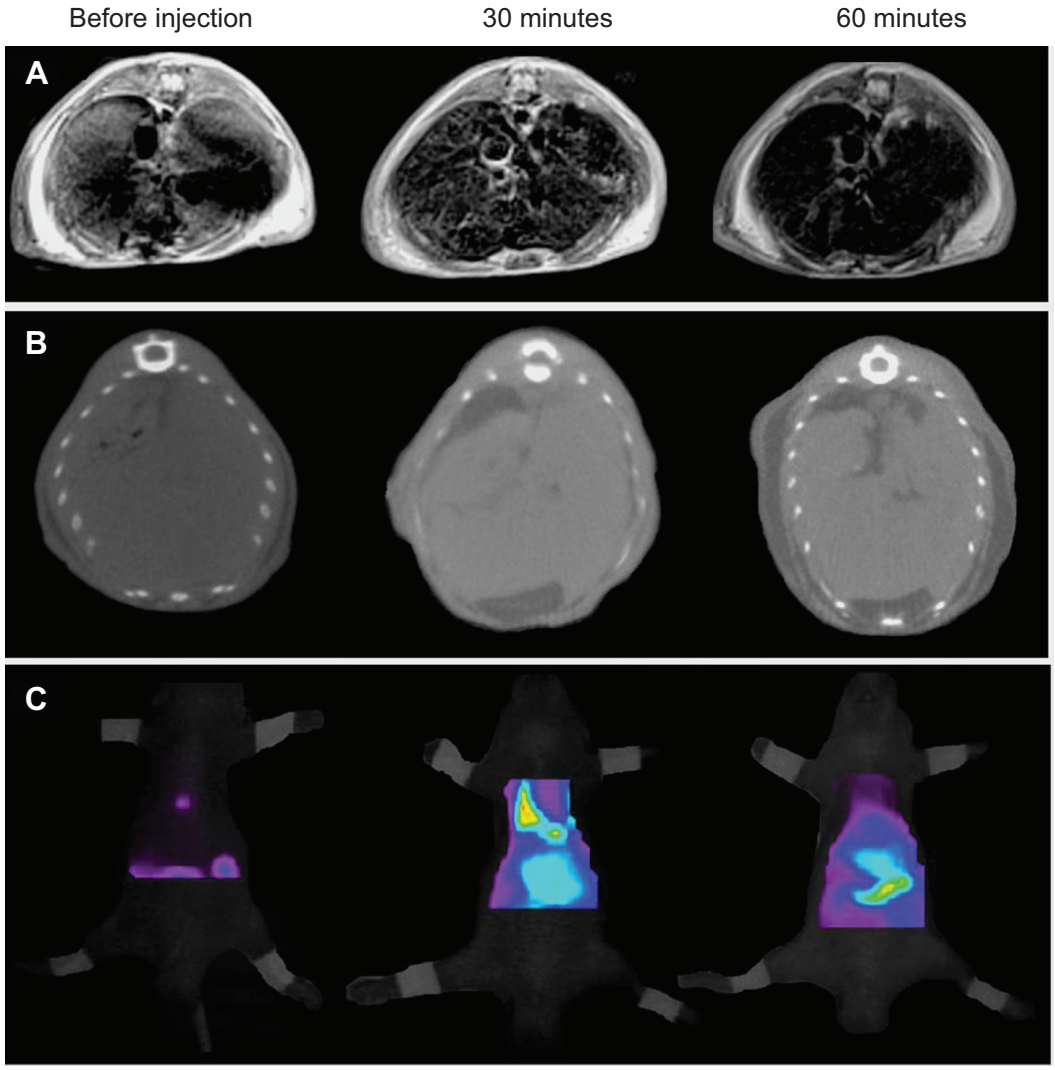

Figure 6 In vivo imaging of i-fmSiO4@SPIONs.
Notes: (**A**) T2-weighted MR, (**B**) CT, and (**C**) fluorescence images of mouse livers after the intravenous injection of i-fmSiO4@SPIONs at different periods of time postinjection.
Abbreviations: i-fmSiO4@SPIONs, iodinated oil-loaded fluorescent mesoporous silica-coated superparamagnetic iron oxide nanoparticles; MR, magnetic resonance; CT, computed tomography.

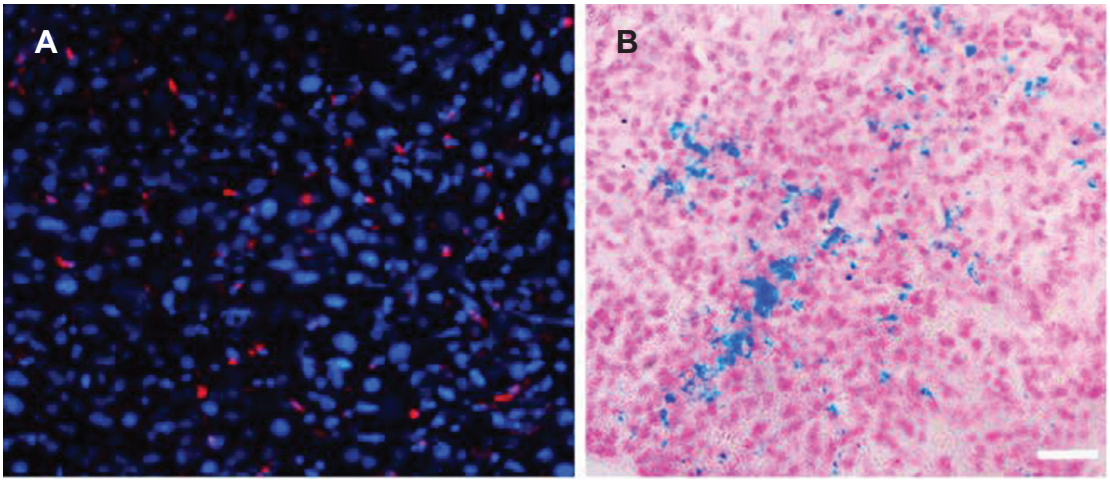

Figure 7 Histological studies of livers.
Notes: (**A**) Fluorescent imaging and (**B**) Prussian blue staining of liver slices. Scale bar: 10 μm.

fluorescence imaging showed that some of the particles were trapped in the lung in the initial 30 minutes, and they had cleared 1 hour post injection.

To verify the existence of the particles in the liver, the mice were sacrificed after imaging and histological studies of liver were performed. As indicated in Figure 7, fluorescent microscopy and Prussian blue staining of liver sections found that there were i-fmSiO4@SPIONs present in the liver.

Conclusion

In summary, we have fabricated a novel MRI/CT/fluorescence trifunctional probe by loading iodinated oil into fmSiO4@SPIONs. I-fmSiO4@SPIONs were biocompatible and they demonstrated good MRI/CT/fluorescence properties both in vitro and in vivo. I-fmSiO4@SPIONs have great potential for MRI/CT/fluorescence trimodal imaging.

Acknowledgments

This research was supported by the Major State Basic Research Development Program of China (973 Program) (Number 2010CB834303, 2010CB933901), National Nature Science Foundation of China (81230030, 30870682), and the Med-Engineering Crossing Foundation of Shanghai Jiao Tong University (YG2011ZD07, YG2012MS15).

Disclosure

The authors report no conflicts of interest in this work.

References

1. Margolis DJ, Hoffman JM, Herfkens RJ, Jeffrey RB, Quon A, Gambhir SS. Molecular imaging techniques in body imaging. *Radiology*. 2007;245(2):333–356.
2. Kircher MF, Willmann JK. Molecular body imaging: MR imaging, CT, and US. Part II. Applications. *Radiology*. 2012;264(2):349–368.
3. Lusic H, Grinstaff MW. X-ray-computed tomography contrast agents. *Chem Rev*. 2013;113(3):1641–1666.
4. Liu Y, Yang Y, Zhang C. A concise review of magnetic resonance molecular imaging of tumor angiogenesis by targeting integrin αvβ3 with magnetic probes. *Int J Nanomedicine*. 2013;8:1083–1093.
5. James ML, Gambhir SS. A molecular imaging primer: modalities, imaging agents, and applications. *Physiol Rev*. 2012;92(2):897–965.
6. Ding J, Wang Y, Ma M, et al. CT/fluorescence dual-modal nanoemulsion platform for investigating atherosclerotic plaques. *Biomaterials*. 2013;34(1):209–216.
7. Chen Q, Li K, Wen S, et al. Targeted CT/MR dual mode imaging of tumors using multifunctional dendrimer-entrapped gold nanoparticles. *Biomaterials*. 2013;34(21):5200–5209.
8. Hu DH, Sheng ZH, Zhang PF, et al. Hybrid gold-gadolinium nanoclusters for tumor-targeted NIRF/CT/MRI triple-modal imaging in vivo. *Nanoscale*. 2013;5(4):1624–1628.
9. Zhang Y, Zhang B, Liu F, Luo J, Bai J. In vivo tomographic imaging with fluorescence and MRI using tumor-targeted dual-labeled nanoparticles. *Int J Nanomedicine*. 2014;9:33–41.
10. Gai S, Li C, Yang P, Lin J. Recent progress in rare earth micro/nanocrystals: soft chemical synthesis, luminescent properties, and biomedical applications. *Chem Rev*. 2014;114(4): 2343−2389.
11. Dong W, Li Y, Niu D, et al. A simple route to prepare monodisperse Au NP-decorated, dye-doped, superparamagnetic nanocomposites for optical, MR, and CT trimodal imaging. *Small*. 2013;9(15): 2500–2508.
12. Hemmer E, Venkatachalam N, Hyodo H, et al. Upconverting and NIR emitting rare earth based nanostructures for NIR-bioimaging. *Nanoscale*. 2013;5(23):11339–11361.
13. Xia A, Chen M, Gao Y, Wu D, Feng W, Li F. Gd3+ complex-modified NaLuF4-based upconversion nanophosphors for trimodality imaging of NIR-to-NIR upconversion luminescence, X-ray computed tomography and magnetic resonance. *Biomaterials*. 2012;33(21):5394–5405.
14. Liu Z, Pu F, Huang S, Yuan Q, Ren J, Qu X. Long-circulating Gd(2)O(3):Yb(3+), Er(3+) up-conversion nanoprobes as high-performance contrast agents for multi-modality imaging. *Biomaterials*. 2013;34(6):1712–1721.
15. Xing H, Bu W, Zhang S, et al. Multifunctional nanoprobes for upconversion fluorescence, MR and CT trimodal imaging. *Biomaterials*. 2012;33(4):1079–1089.
16. Zeng S, Tsang MK, Chan CF, Wong KL, Hao J. PEG modified $BaGdF_5$:Yb/Er nanoprobes for multi-modal upconversion fluorescent, in vivo X-ray computed tomography and biomagnetic imaging. *Biomaterials*. 2012;33(36):9232–9238.

17. Zheng J, Perkins G, Kirilova A, Allen C, Jaffray DA. Multimodal contrast agent for combined computed tomography and magnetic resonance imaging applications. *Invest Radiol*. 2006;41(3):339–348.
18. Zheng J, Liu J, Dunne M, Jaffray DA, Allen C. In vivo performance of a liposomal vascular contrast agent for CT and MR-based image guidance applications. *Pharm Res*. 2007;24(6):1193–1201.
19. Li X, Xie QR, Zhang J, Xia W, Gu H. The packaging of siRNA within the mesoporous structure of silica nanoparticles. *Biomaterials*. 2011; 32(35):9546–9556.
20. Li X, Chen Y, Wang M, Ma Y, Xia W, Gu H. A mesoporous silica nanoparticle – PEI – fusogenic peptide system for siRNA delivery in cancer therapy. *Biomaterials*. 2013;34(4):1391–1401.
21. Zhang J, Li X, Rosenholm JM, Gu HC. Synthesis and characterization of pore size-tunable magnetic mesoporous silica nanoparticles. *J Colloid Interface Sci*. 2011;361(1):16–24.
22. Liu Q, Zhang J, Sun W, Xie QR, Xia W, Gu H. Delivering hydrophilic and hydrophobic chemotherapeutics simultaneously by magnetic mesoporous silica nanoparticles to inhibit cancer cells. *Int J Nanomedicine*. 2012;7:999–1013.
23. Zhang L, Wang Y, Tang Y, et al. High MRI performance fluorescent mesoporous silica-coated magnetic nanoparticles for tracking neural progenitor cells in an ischemic mouse model. *Nanoscale*. 2013;5(10):4506–4516.
24. Zhang J, Rosenholm JM, Gu H. Molecular confinement in fluorescent magnetic mesoporous silica nanoparticles: effect of pore size on multifunctionality. *Chemphyschem*. 2012;13(8):2016–2019.
25. Brunauer S, Emmett PH, Teller E. Adsorption of gases in multimolecular layers. *J Am Chem Soc*. 1938;60:309–319.
26. Ravikovitch PI, Wei D, Chueh WT, Haller GL, Neimark AV. Evaluation of pore structure parameters of MCM-41 catalyst supports and catalysts by means of nitrogen and argon adsorption. *J Phys Chem B*. 1997;101(19):3671–3679.
27. Barrett EP, Joyner LG, Halenda PP. The determination of pore volume and area distributions in porous substances. I. Computations from nitrogen isotherms. *J Am Chem Soc*. 1951;73(1):373–380.
28. Zhang C, Xie X, Liang S, Li M, Liu Y, Gu H. Mono-dispersed high magnetic resonance sensitive magnetite nanocluster probe for detection of nascent tumors by magnetic resonance molecular imaging. *Nanomedicine: NBM*. 2012;8(6):996–1006.
29. Zhang Y, Yang Y, Cai W. Multimodality Imaging of Integrin $\alpha(v)\beta(3)$ Expression. *Theranostics*. 2011;1:135–148.
30. van Schooneveld MM, Cormode DP, Koole R, et al. A fluorescent, paramagnetic and PEGylated gold/silica nanoparticle for MRI, CT and fluorescence imaging. *Contrast Media Mol Imaging*. 2010;5(4): 231–236.
31. Kim T, Momin E, Choi J, et al. Mesoporous silica-coated hollow manganese oxide nanoparticles as positive T1 contrast agents for labeling and MRI tracking of adipose-derived mesenchymal stem cells. *J Am Chem Soc*. 2011;133(9):2955–2961.
32. Kim J, Kim HS, Lee N, et al. Multifunctional uniform nanoparticles composed of a magnetite nanocrystal core and a mesoporous silica shell for magnetic resonance and fluorescence imaging and for drug delivery. *Agnew Chem Int Ed Engl*. 2008;47(44): 8438–8441.
33. Kim D, Yu MK, Lee TS, Park JJ, Jeong YY, Jon S. Amphiphilic polymer-coated hybrid nanoparticles as CT/MRI dual contrast agents. *Nanotechnology*. 2011;22(15):155101.
34. Jeong JM, Kim YJ, Lee YS, et al. Lipiodol solution of a lipophilic agent, (188)Re-TDD, for the treatment of liver cancer. *Nucl Med Biol*. 2001;28(2):197–204.
35. Yamagami T, Masunami T, Kato T, et al. Spontaneous healing of chyle leakage after lymphangiography. *Br J Radiol*. 2005;78(933): 854–857.
36. Kong WH, Lee WJ, Cui ZY, et al. Nanoparticulate carrier containing water-insoluble iodinated oil as a multifunctional contrast agent for computed tomography imaging. *Biomaterials*. 2007;28(36):5555–5561.
37. Hallouard F, Anton N, Choquet P, Constantinesco A, Vandamme T. Iodinated blood pool contrast media for preclinical X-ray imaging applications – a review. *Biomaterials*. 2010;31(24):6249–6268.
38. Kweon S, Lee HJ, Hyung WJ, Suh J, Lim JS, Lim SJ. Liposomes coloaded with iopamidol/lipiodol as a RES-targeted contrast agent for computed tomography imaging. *Pharm Res*. 2010;27(7):1408–1415.
39. Vallet-Regí M, Balas F, Arcos D. Mesoporous materials for drug delivery. *Angew Chem Int Ed Engl*. 2007;46(40):7548–7558.
40. Lu J, Liong M, Zink JI, Tamanoi F. Mesoporous silica nanoparticles as a delivery system for hydrophobic anticancer drugs. *Small*. 2007;3(8):1341–1346.
41. Rosenholm JM, Sahlgren C, Lindén M. Towards multifunctional, targeted drug delivery systems using mesoporous silica nanoparticles – opportunities and challenges. *Nanoscale*. 2010;2(10):1870–1883.
42. Rosenholm JM, Sahlgren C, Lindén M. Multifunctional mesoporous silica nanoparticles for combined therapeutic, diagnostic and targeted action in cancer treatment. *Curr Drug Targets*. 2011;12(8):1166–1186.
43. Li C, Yang D, Ma P, et al. Multifunctional upconversion mesoporous silica nanostructures for dual modal imaging and in vivo drug delivery. *Small*. 2013;9(24):4150–4159.
44. Douroumis D, Onyesom I, Maniruzzaman M, Mitchell J. Mesoporous silica nanoparticles in nanotechnology. *Crit Rev Biotechnol*. 2013;33(3):229–245.
45. Tarn D, Ashley CE, Xue M, Carnes EC, Zink JI, Brinker CJ. Mesoporous silica nanoparticle nanocarriers: biofunctionality and biocompatibility. *Acc Chem Res*. 2013;46(3):792–801.
46. Rosenholm JM, Mamaeva V, Sahlgren C, Lindén M. Nanoparticles in targeted cancer therapy: mesoporous silica nanoparticles entering preclinical development stage. *Nanomedicine (Lond)*. 2012;7(1):111–120.
47. Blechinger J, Bauer AT, Torrano AA, Gorzelanny C, Bräuchle C, Schneider SW. Uptake kinetics and nanotoxicity of silica nanoparticles are cell type dependent. *Small*. 2013;9(23):3970–3980, 3906.
48. Chuang SM, Lee YH, Liang RY, et al. Extensive evaluations of the cytotoxic effects of gold nanoparticles. *Biochim Biophys Acta*. 2013;1830(10):4960–4973.
49. Rauch J, Kolch W, Laurent S, Mahmoudi M. Big signals from small particles: regulation of cell signaling pathways by nanoparticles. *Chem Rev*. 2013;113(5):3391–3406.
50. Weissleder R, Pittet MJ. Imaging in the era of molecular oncology. *Nature*. 2008;452(7187):580–589.
51. Almeida JP, Chen AL, Foster A, Drezek R. In vivo biodistribution of nanoparticles. *Nanomedicine (Lond)*. 2011;6(5):815–835.
52. Gallo J, Long NJ, Aboagye EO. Magnetic nanoparticles as contrast agents in the diagnosis and treatment of cancer. *Chem Soc Rev*. 2013;42(19):7816–7833.

Supplementary materials

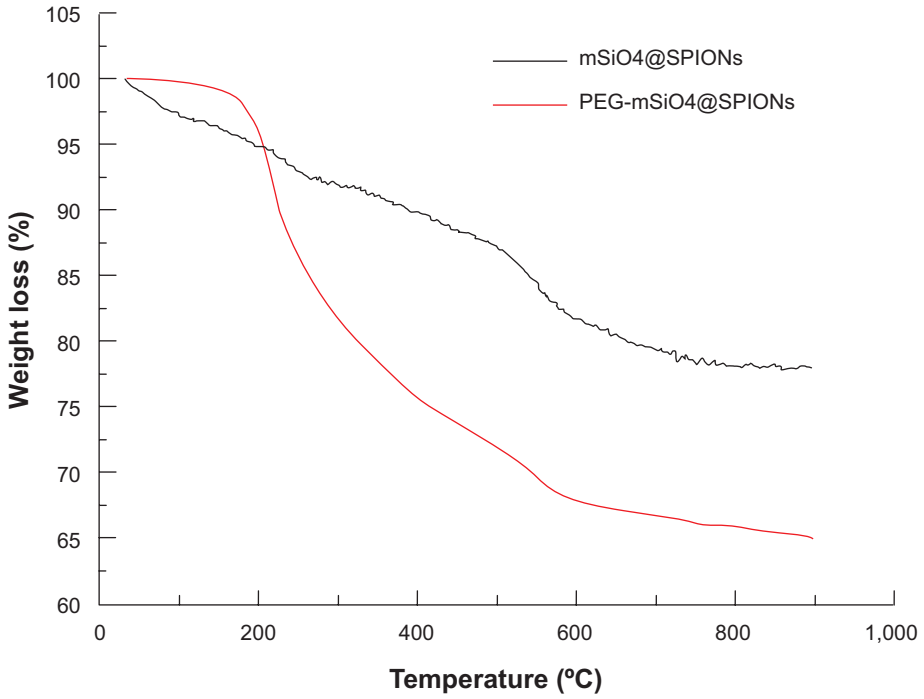

Figure S1 Thermogravimetric analysis of fmSiO4@SPIONs after PEG modification.
Note: After PEG modification, about 13% of weight loss was observed.
Abbreviations: mSiO4@SPIONs, mesoporous silica-coated superparamagnetic iron oxide nanoparticles; PEG, polyethylene glycol; fmSiO4@SPIONs, fluorescent mesoporous silica-coated superparamagnetic iron oxide nanoparticles.